arXiv:1512.07406v2 [cond-mat.quant-gas] 30 Jan 2016

Exotic superfluid of trapped Fermi gases with spin-orbit coupling in dimensional crossover

Jing Zhou,[1,2] Cheng Shi,[1] Xiang-Fa Zhou,[3] Lin Wen,[4] Peng Chen,[1] and Deng-Feng Li[1]

[1] *Department of Science, Chongqing University of Posts and Telecommunications,Chongqing 400065, China*
[2] *Beijing National Laboratory for Condensed Matter Physics, Institute of Physics, Chinese Academy of Sciences, Beijing 100190, China*
[3] *Key Laboratory of Quantum Information, University of Science and Technology of China, CAS, Hefei, Anhui, 230026, People's Republic of China*
[4] *College of Physics and Electronic Engineering, Chongqing Normal University, Chongqing, 401331, China*

We have studied the exotic superfluid phases of degenerated Fermi gases with spin-orbit coupling in a mixed dimensional system, where the motion of atoms are free in the $\hat{x}$-direction and the tunneling between nearest tubes in the $\hat{y}$-direction is permitted. Using the mean-field method, we obtain the phase diagrams of the system during the dimensional crossover between quasi one dimension to quasi two dimension. We find the existence of the topological state and Majorana edge mode in the weak tunneling case, and a rich phase diagram including two kinds of nodal superfluid phase and gapped superfluid phase in the opposite case. Our results show that topological pairing is favoured in quasi one dimension while nodal pairing state is favoured in quasi two dimension.

PACS numbers: 03.75.Ss, 03.75.Lm, 67.85.Lm

I. INTRODUCTION

Spin-orbit coupling (SOC) has received tremendous attention due to its rich physics. For instance, it gives rise to novel transport properties in semiconductor materials [1–3], and plays a crucial role in the formation of many important phenomena including topological insulator [4], topological conductor [5], and quantum spin Hall effect [6]. In recent years, with the help of Raman laser coupling, SOC has been implemented experimentally [7–9] in ultra-cold neutral atomic system and has attracted considerable attentions both theoretically and experimentally [10–29]. Due to its highly flexibility, cold atom system is considered as an ideal platform for the quantum simulation of interesting physics models, ranging from nuclear physics [30, 31] to condensed matter physics [32, 33]. This provides a great opportunity to investigate such novel SOC physics in a highly controllable way.

Fulde-Ferrell-Larkin-Ovchinnikov (FFLO) state first proposed in the 1960s [34, 35] is an exotic superfluid pairing state with finite momentum compared with the conventional superconductor with zero momentum pairing. In general, FFLO state emerges with mismatched fermi surface of imbalanced Fermi gas. Therefore, it has been viewed as one of the most interesting superconduction phases, and is studied in various field, ranging from heavy fermions [36–38], organic superconductor [39] to ultracold atomic gases [40–45]. However, due to the small pairing phase space in 2D and 3D, only phase separation is observed in experiments rather than FFLO state. The difficulty is avoided in 1D system, where the fermi surface is point, and the pairing phase space isn't affected by the spin imbalanced. But the large quantum fluctuation in 1D might suppress the long-range order. With spin-orbit coupling and Zeeman field, the spatial inversion symmetry is broken and paring on a single Fermi surface is passible. Theoretical investigation indicates that FFLO state is favoured in this system with nontrivial topology [46–49].

In this paper, we consider an array of Fermi tubes with one dimension SOC. The atoms can move freely along the $\hat{x}$-direction while nearest tube tunneling is allowed in our model [50]. The tunneling can be adjusted over a wide range by tuning the optical lattice height in the $\hat{y}$-direction so that we can realize the crossover from quasi one dimensional system to quasi two dimensional ones. With different tunneling strength, we obtain the mean-field ground state, and confirm that the FFLO state is hosted in such dimensional crossover system. Furthermore, we show topological FFLO state is more stable with smaller tunneling, which can be verified by the appearance of typical Majorana zero mode. To obtain the phase transition point between topological FFLO state and normal FFLO state, we use two coupled tubes model to analyze the phase transition and find the critical tunneling. It indicates that topological FFLO state exists not only in 1D [23, 27], but also in quasi 1D. For quasi two dimensional system, we find the system supports novel gapless superfluid phases which can be classified by the number of gapless points in the excitation spectra. The influence of transverse Zeeman field, interaction strength, and tunneling between nearest tubes on these novel phases are also studied. Detailed calculation shows that the presence of transverse Zeeman field eradicates the zero center-of-mass momentum pairing, and stabilizes nodal FFLO state with finite center-of-mass momentum pairing along anisotropic SOC direction. We also give the phase diagrams with different interactions and tunneling and show the interaction effect and how the crossover physics can be explored by tuning the tunneling.

The rest of this paper is organized as follows: in the next section (Sec.II), we introduce our model and detailed calculation method based on the standard

Bogoliubov-de Gennes (BdG) theory. In Sec.III, we discuss the phase diagram of quasi one dimensional system with small inter-tube tunneling. Two coupled tubes model is used to analyze the critical tunneling between topological FFLO state and normal FFLO state, where topological properties can be verified by the presence of Majorana edge modes. In Sec. IV, we investigate the phase diagram of quasi two dimensional system. The effects of transverse Zeeman field, interaction and tunneling are studied to capture the properties of the exotic nodal superfluid states, where the crossover physics can also be clearly manifested. Finally, we summarize the results and draw our conclusion in Sec. V.

II. MODEL HAMILTONIAN AND CALCULATION METHOD

We start by considering two-component Fermi gas with SOC and Zeeman field in an array of tubes. As shown in Fig.1, the red tubes are parallel to the $\hat{x}$-direction. Two counter-propagating laser lights along the $\hat{y}$-direction construct one dimension optical lattice in this direction. The tunneling between nearest tubes is permitted in the model. The type of SOC is induced by another two counter-propagating Raman laser lights along $\hat{x}$-direction. The Hamiltonian can be written as

$$H-\sum_{\sigma}\mu_{\sigma}N_{\sigma}=H_0+H_{SOC}+H_{Zee}+H_{int}, \qquad (1)$$

with

$$\begin{aligned}
H_0 &= \sum_{\sigma,k_x,j}\varepsilon_k C^{\dagger}_{k_xj\sigma}C_{k_xj\sigma}-t\sum_{\sigma,k_x,\langle i,j\rangle}C^{\dagger}_{k_xi\sigma}C_{k_xj\sigma}+h.c.,\\
H_{SOC} &= \sum_{k_x,j}(\alpha k_x C^{\dagger}_{k_xj\uparrow}C_{k_xj\uparrow}-\alpha k_x C^{\dagger}_{k_xj\downarrow}C_{k_xj\downarrow}),\\
H_{Zee} &= \sum_{k_x,j}h_x(C^{\dagger}_{k_xj\uparrow}C_{k_xj\downarrow}+C^{\dagger}_{k_xj\downarrow}C_{k_xj\uparrow}),\\
&\quad -h(C^{\dagger}_{k_xj\uparrow}C_{k_xj\uparrow}-C^{\dagger}_{k_xj\downarrow}C_{k_xj\downarrow}),\\
H_{int} &= g\sum_{\mathbf{k},\mathbf{k}',\mathbf{Q}}C^{\dagger}_{\mathbf{k}+\mathbf{Q}/2\uparrow}C^{\dagger}_{-\mathbf{k}+\mathbf{Q}/2\downarrow}C_{-\mathbf{k}'+\mathbf{Q}/2\downarrow}C_{\mathbf{k}'+\mathbf{Q}/2\uparrow},
\end{aligned}$$

where $\varepsilon_k=\frac{\hbar^2k_x^2}{2m}-\mu$, $C_{k_x\sigma j}$ ($C^{\dagger}_{k_x\sigma j}$) is the annihilation (creation) operator for the hyperfine spin state σ in the j-th tube. m is the atom mass, α denotes the strength of the SOC, t is the near-rest tunneling between different tubes, and $h.c.$ represents the Hermitian conjugate. The Zeeman field contains two terms: in-plane (h_x) and out-of-plane (h) magnetic fields, which are included in the current experimental scheme. g is the bare strength of s-wave attractive interaction.

Throughout the paper, we only focus on the zero temperature properties of the system. The order parameter of FF pairing state is defined as $\Delta_{\mathbf{Q}}=g\sum_{\mathbf{k}}\langle C_{-\mathbf{k}+\mathbf{Q}/2\downarrow}C_{\mathbf{k}+\mathbf{Q}/2\uparrow}\rangle$. Within mean field approximation, we can rewrite the Hamiltonian based on the Nanbu spinor base $\Psi_{\mathbf{k}}=[C_{\mathbf{k}+\mathbf{Q}/2\uparrow},C_{\mathbf{k}+\mathbf{Q}/2\downarrow},C^{\dagger}_{-\mathbf{k}+\mathbf{Q}/2\uparrow},C^{\dagger}_{-\mathbf{k}+\mathbf{Q}/2\downarrow}]^T$ as follows

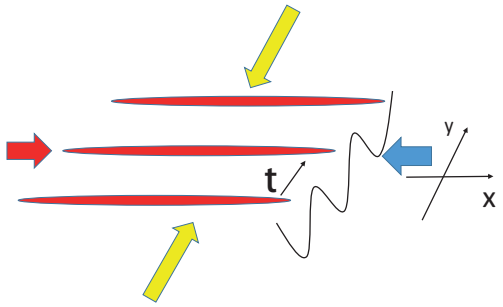

FIG. 1: Illustration of the model in an array of coupled tubes in two-dimensional plane, which can realize dimensional crossover.

$$\hat{H}=\frac{1}{2}\sum_{\mathbf{k}}\hat{\Psi}^{\dagger}_{\mathbf{k}}H_{eff}\hat{\Psi}_{\mathbf{k}}+\sum_{\mathbf{k}}\zeta_{-\mathbf{k}+\mathbf{Q}/2}-\frac{\Delta^2_{\mathbf{Q}}}{g} \qquad (2)$$

with the BdG Hamiltonian

$$H_{eff}=\begin{pmatrix}
\lambda^{+}_{\mathbf{k}+\mathbf{Q}/2} & h_x & 0 & \Delta_{\mathbf{Q}}\\
h_x & \lambda^{-}_{\mathbf{k}+\mathbf{Q}/2} & -\Delta_{\mathbf{Q}} & 0\\
0 & -\Delta_{\mathbf{Q}} & -\lambda^{+}_{-\mathbf{k}+\mathbf{Q}/2} & -h_x\\
\Delta_{\mathbf{Q}} & 0 & -h_x & -\lambda^{-}_{-\mathbf{k}+\mathbf{Q}/2}
\end{pmatrix}, \qquad (3)$$

where $\lambda^{\pm}_{\mathbf{k}}=\hbar^2k_x^2/2m-2t(\cos(k_y)-1)\pm(\alpha k_x-h)$, and $\zeta_k=\hbar^2k_x^2/2m-2t(\cos(k_y)-1)-\mu$. Since there is no constrain in the $\hat{x}$-direction, k_x still remains to be a good quantum number, while k_y is confined in the first Brillouin $|k_y|\leq\pi$. The tunneling t is highly controllable by changing the lattice height in the $\hat{y}$-direction, which allow us to investigate the crossover physics from 1D to 2D.

In order to get the zero temperature phase diagram, we straightforwardly diagonalize the BdG Hamiltonian H_{eff} and calculate the thermodynamic potential $\Omega=-\frac{1}{\beta}\log\mathrm{Tr}e^{-\beta(H-\mu N)}$. For zero temperature, the thermodynamic potential is:

$$\Omega=\sum_{\mathbf{k}}\zeta_{-\mathbf{k}+\mathbf{Q}/2}+\sum_{\mathbf{k},\nu,\eta}\Theta(-E^{\nu}_{\mathbf{k},\eta})E^{\nu}_{\mathbf{k},\eta}-\frac{|\Delta_{\mathbf{Q}}|^2}{g}, \qquad (4)$$

where the quasi-particle (hole) dispersion $E^{\nu}_{\mathbf{k},\eta}$ ($\eta,\nu=\pm$) are the eigenvalues of the BdG Hamiltonian. And Θ is the Heaviside step function. For sake of simplicity, we can assume the order parameter $\Delta_{\mathbf{Q}}$ to be real throughout the whole work. In this model, due to the complex 4×4 matrix H_{eff}, the analytical expression of quasi-particle dispersion $E^{\nu}_{k,\eta}$ are too complicated to be presented here, so we will perform our calculation numerically. In general, the ground state can be obtained from

the saddle point equations $\partial\Omega/\partial\Delta = 0$, $\partial\Omega/\partial\mathbf{Q} = 0$ and $\partial\Omega/\partial\mu = -n$. However, Due to the competition between pairing and the Zeeman field, the thermodynamic potential shows double well structure. We may get metastable state from the gap equation. In order to find the true ground state, we numerically search for the global minimum of the thermodynamic potential to obtain the order parameter $\Delta_{\mathbf{Q}}$ as well as the finite mass momentum $\mathbf{Q}$. We note that in our work, the phase diagram is obtained by fixing the chemical potential throughout the whole system. For a trapped gas system, the local chemical potential is defined as $\mu(\mathbf{r}) = \mu - V(\mathbf{r})$, which is known as the local density approximation (LDA). In principle, based on our calculation, we can sweep chemical potential to obtain the phase structure in a trapped system. The total particle number can be evaluated by integrating the local particle density from the trap center to the edge.

III. QUASI ONE DIMENSIONAL RESULT

A. PHASE DIAGRAM

For the fixed chemical potential, the paring order parameter is obtained by searching the global minimum of the thermodynamic potential. In the calculation, we find with not large enough h, FF state with finite paring momentum $\mathbf{Q} = Q\widehat{x}$ is stable in a fairly large parameter region. We map out the phase diagram in $\alpha - \mu$ plane, where a topological FF phase (tFF) is always sandwiched between a normal FF state (gFF) and normal state (N) without pairing.

The tFF state can be understood from the symmetry of the BdG Hamiltonian

$$H_{BdG}(\mathbf{k}) = \begin{pmatrix} \lambda^{+}_{\mathbf{k+Q/2}} & h_x & 0 & \Delta_{\mathbf{Q}} \\ h_x & \lambda^{-}_{\mathbf{k+Q/2}} & -\Delta_{\mathbf{Q}} & 0 \\ 0 & -\Delta_{\mathbf{Q}} & -\lambda^{+}_{\mathbf{-k+Q/2}} & -h_x \\ \Delta_{\mathbf{Q}} & 0 & -h_x & -\lambda^{-}_{\mathbf{-k+Q/2}} \end{pmatrix}. \tag{5}$$

We note that this Hamiltonian processes a particle-hole symmetry as $\Xi H_{BdG}\Xi^{-1} = \Lambda H^{*}_{BdG}(\mathbf{k})\Lambda = -H_{BdG}(-\mathbf{k})$. Here, $\Xi = \Lambda K$, $\Lambda = (\sigma_y\tau_y)$ and K is the complex conjugation operator. $\sigma_{x,y,z}$ are the Pauli-spin matrices and $\tau_{x,y,z}$ are the Nanbu particle-hole matrices. In this case, the topological character is verified by the topological number - Pfaffian invariant Q [53], which can in principle be computed in terms of the eigenvalues of $H_{BdG}(\mathbf{k})$. The topological phase corresponds to $Q = -1$, while the topological trivial state corresponds to $Q = 1$. In general, the topological nature is protected by the gap in the bulk quasi-particle excitation. The phase boundary between tFF state and gFF state can be determined by the gap condition. According to the symmetry, the gap closes at a single point $\mathbf{k} = (0, 0)$. With simple matrix determinate calculation, we find the energy gap close and reopen condition is

$$h^2 = \Delta^2_{\mathbf{Q}} - h_x^2 + \alpha h Q_x - \frac{1}{4}\alpha^2 Q_x^2 + (\mu - \frac{Q_x^2}{4})^2. \tag{6}$$

In the special case that both the in-plane Zeeman field h_x and the paring momentum Q_x equals to zero, the above formula reduces to the standard condition for BCS topological superfluid $h^2 = \Delta^2 + \mu^2$ [15].

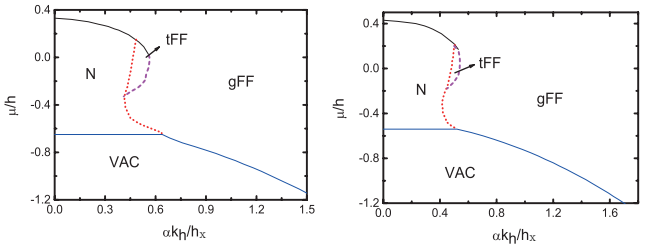

FIG. 2: The phase diagram in the $\alpha - \mu$ plane with different tunneling t (Left: $t = 0.02$; Right: $t = 0.08$). The first order phase transition is shown in black solid line while the topological phase transition in dashed burgundy curve. The red dotted line marks the $\Delta/h_x = 10^{-3}$ threshold. The in-plane Zeeman field is taken as the energy unit, while the unit of momentum k_h is defined through $\hbar^2 k_h^2/2m = h_x$. The other parameters used in this plot are:$g/h_x = -0.5, h/h_x = 0.2$.

In Fig. 2, we show the phase diagrams of quasi-1D system, where the first order phase transition is shown in black solid line while the topological phase transition is shown in dashed burgundy curve. The red dotted line marks the $\Delta/h_x = 10^{-3}$ threshold. The phase boundary between gFF state and normal state is determined from the double well structure of the thermodynamic potential. The tFF state in the phase diagram is verified by the topological invariant Pfaffian and the topological condition above. Comparing the two plots in Fig. 2, it is obvious that tFF state region is much larger with weaker tunneling t. This means that tFF state of our system is much more stable in quasi one dimensional geometry than in quasi two dimensional one.

B. TWO COUPLED TUBES MODEL

To investigate the effect of tunneling on phase transition, we further consider a simplified toy model with only two coupling tubes. Within mean-field approximation, we calculate the elementary excitations using the standard Bogoliubov-de Gennes equation as

$$H_{BdG}(x)\Psi(x) = E_n\Psi(x), \tag{7}$$

where $\Psi(x) = [u^{\uparrow}_{n,1}, u^{\downarrow}_{n,1}, u^{\uparrow}_{n,2}, u^{\downarrow}_{n,2}, v^{\uparrow}_{n,1}, v^{\downarrow}_{n,1}, v^{\uparrow}_{n,2}, v^{\downarrow}_{n,2}]^T$. The paring parameter of i-th tube is defined as $\Delta(x)^i = g\sum_n(u^{\downarrow}_{n,i}v^{\uparrow *}_{n,i}f(-E_n) + v^{\downarrow *}_{n,i}u^{\uparrow}_{n,i}f(E_n))$. $f(x) = 1/(e^{x/k_BT} + 1)$ is the Fermi distribution at temperature T. For zero temperature, the Fermi distribution reduces

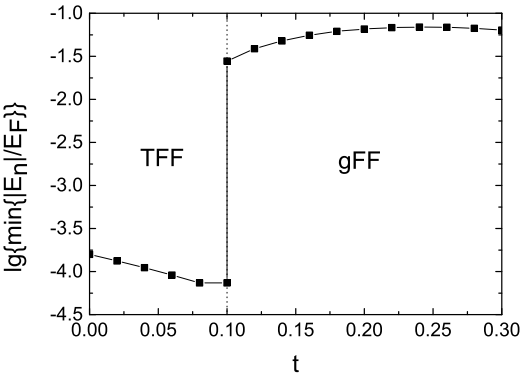

FIG. 3: Phase diagram for a given spin-orbit coupling $\alpha k_F/E_F = 0.6$ of two coupled tubes model, is determined from the real space BdG calculation. The Bogoliubov excitation spectra is calculated by diagonalizing a large matrix in the real space. As tunneling increases, a phase transition occurs, and the system evolves from a tFF state to a gFF state. The critical tunneling $t = 0.1$. The other parameter is set as: $g = -0.3, h = 0.2, hx = 0.2, \alpha k_F/E_F = 0.6$. The energy unit E_F is determined by the total particle number.

to $f(x) = \Theta(-x)$ with Θ being the heaviside function. The particle number of i-th tube and spin σ component is $n_i^\sigma = \sum_n (|u_{n,i}^\sigma|^2 f(E_n) + |v_{n,i}^\sigma| f(-E_n))$. In order to get the information of the wave functions in real space, we expand the wave function as

$$u_{n,i}^{\uparrow} = \sum_m A_{n,m}^{\uparrow,i} \sqrt{\frac{2}{L}} \sin(\frac{m\pi x}{L}), \tag{7a}$$

$$u_{n,i}^{\downarrow} = \sum_m A_{n,m}^{\downarrow,i} \sqrt{\frac{2}{L}} \sin(\frac{m\pi x}{L}), \tag{7b}$$

$$v_{n,i}^{\uparrow} = \sum_m B_{n,m}^{\uparrow,i} \sqrt{\frac{2}{L}} \sin(\frac{m\pi x}{L}), \tag{7c}$$

$$v_{n,i}^{\downarrow} = \sum_m B_{n,m}^{\downarrow,i} \sqrt{\frac{2}{L}} \sin(\frac{m\pi x}{L}). \tag{7d}$$

In our calculation, the cutoff number of the base function is set to be $N_c = 300$. The absolute value of the minimum excitation energy with different t is shown in Fig. 3. We find that, when t is below 0.1, the absolute value of the minimum of the Bogoliubov energy is quite small (about 10^{-4}), while absolute value of the minimum energy changes to be $\sim 10^{-1}$ with tunneling above 0.1. An obvious leap emerges at a critical value $t = 0.1$. This signifies the phase transition between tFF state and gFF state.

Figure 4 shows the energy spectra and the wave functions of tFF state and gFF state with different tunneling parameters. In the case of tFF phase with $t = 0.05$, there are zero modes in subgraph (a), which is known as the Majorana fermion, and signifies the topological property

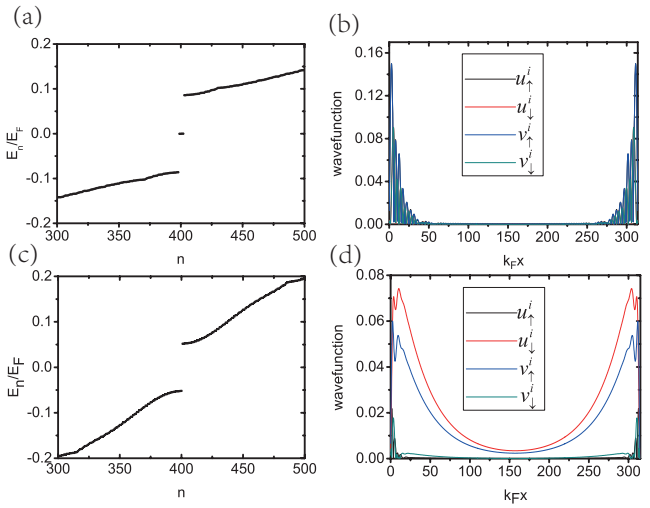

FIG. 4: Bogoliubov spectra and wave functions with different tunneling are shown in this figure. For our two coupled tubes model, when $t = 0.05$, there is zero mode in the spectra (in (a)), which is known as majorana fermion. And the wave function in (b) shows edge mode in this case. In contrast, the spectra is fully gapped if $t = 0.15$. And the wave function is extensional in (d). The other parameter of this figure is set as:$g = -0.3, h = 0.2, hx = 0.2, \alpha k_F/E_F = 0.6$. The Fermi energy E_F is determined by the total particle number.

in this state. The corresponding eigen wave function in real space is also depicted in Fig.4(b), which is localized at the edge of the $\hat{x}$-direction. We note that owing to the symmetry of tube 1 and tube 2, only the edge mode in the first tube is shown. When $t = 0.15$, which is larger than the critical point, the spectra is fully gapped as shown in subplot (c). And the corresponding wave function (subgraph (d)) is more extended contrast with subgraph (b).

In conclusion, we get qualitative result of the phase transition with different tunneling. When t is small, the array of the coupling tubes is similar to quasi one dimensional system. We show the topological phase and topological elementary excitation. If we tune the tunneling larger, the model is more like quasi two dimensional system. And the system is fully gapped. With two coupled tubes model approximation, we get the critical point of the phase transition.

IV. QUASI TWO DIMENSIONAL RESULT

A. PAIRING STATE WITH ZERO CENTER OF MASS MOMENTUM

In last section, we analyze the phase diagrams and the topological state with weak tunneling t. To get a better understanding about the crossover physics, in this section, we focus on the quasi two dimensional geometry

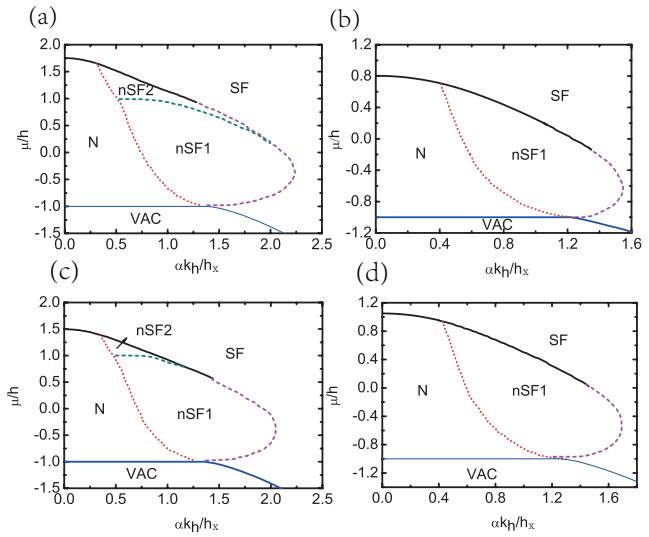

FIG. 5: Phase diagrams with different interaction g and different tunneling t on the $\alpha-\mu$ plane . For (a) and (b), the parameter is set as: (a).$g=-0.35, t=1$;(b).$g=-0.65, t=1$, respectively. For (c) and (d), the parameter is set as: (c).$g=-0.35, t=0.9$; (d).$g=-0.35, t=0.7$, respectively. In all the figures, the black solid lines represent the first-order phase transition boundaries while the dashed burgundy lines represent the continuous phase transition boundaries. The red dotted curve corresponds to $\Delta=10^{-3}$ threshold. $h=1$ in all the subplots.

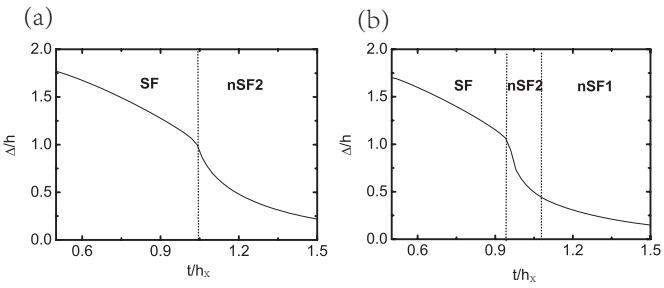

FIG. 6: Phase diagrams with different tunneling t. The chemical potential μ in (a) and (b) is set as $\mu=0.6$ and $\mu=0.9$, respectively. The other parameters are set as follows: $g=-0.3; \lambda k_h/h_x=1.2, h_x=1, h=0$.

where the tunneling t can be changed over a wide parameter range. We start by studying the pairing states with zero out-of-plane Zeeman field. When $h=0$, H_{eff} can be diagonalized analytically. It can be verified numerically that in this case, paring with zero center-of-mass momentum $Q_x=0$ is stable against finite momentum paring. The analytical expression of the quasi-particle and quasi-hole dispersions along $k_x=0$ axis can be written as $E^{\lambda}_{k_x=0,\pm}=\lambda(\sqrt{\varepsilon^2_{ky}+\Delta^2}\pm h_x)$ with $\lambda=\pm$, and $\varepsilon_{ky}=-2t(cos(k_y)-1)$. Apparently, only two of the branchs $E^{\lambda}_{k_x=0,-}$ can cross zero. And this leads to the exotic nodal superfluid (nSF) with gapless points in the excitation spectra. It is interesting to classify nSF state with different number of gapless points. Typically, there can be two kinds of nSF state with two or four isolated gapless points. A simple calculation shows that when $\mu\pm\sqrt{h_x^2-\Delta^2}\in[0,4t]$, there will be four isolated gapless points in the excitation spectra, while the excitation spectra is fully gapped when$\mu\pm\sqrt{h_x^2-\Delta^2}\notin[0,4t]$. Otherwise, we find that only two gapless points appear in the dispersion.

In Fig. 5, we map out the phase diagram with different interaction g on the $\alpha-\mu$ plane. Compared with phase diagrams with Rashba SOC in two dimension [16], the topological phase is now replaced by nodal superfluid state. We focus on nodal superfluid in our quasi two dimensional model. With anisotropic SOC, superfluid state with zero center-of mass momentum pairing is still stable against normal state with a large in-plane Zeeman field h_x. As we have anticipated, there exists two kinds of nodal superfluid states with either four isolated nodes or two isolated nodes in the excitation spectra as shown in Fig. 5(a). The four-node superfluid disappears in Fig. 5(b) as we increase the interaction strength to $g=-0.65$. It means that the nodal superfluid is more stable with weaker interaction. To study the phase transition in the case of dimensional crossover from 1D to 2D, we also plot the phase diagrams with different tunneling t as shown in subgraphs (a,c,d) of Fig. 5. For fixed interaction strength $g=-0.35$, one can see that the four-nodal superfluid region shrinks rapidly and finally disappears from the phase diagram with $t=0.7$ (Fig. 5d). Therefore, the four-nodal phase is more stable with relatively larger ratio $|t/g|$. We note that in these cases, nodal phases process a relatively large region. This is very different from the quasi one dimensional case, where gFF state dominates the superfluid region, and tFF state disappears very quickly as we increase the inter-tube tunneling. Therefore, we can claim that nodal-superfluid is more stable in quasi two dimensional geometry than the quasi one dimensional case.

To illustrate the crossover behaviors of the SF phases along with the tunneling, we also plot the evolution of pairing parameter Δ as a function of t/h_x from 0.5 to 1.5 by fixing all other parameters. As shown in Fig. 6(a), one can see below a critical tunneling value $t_c/h_x=1.04$, Δ changes smoothly. This corresponds to the normal paring state and the excitation spectra is gapped. However, the gap closes and the ground state changes to a four-node paring phase (nSF2) when the tunneling is above the critical value. This transition is of first-order which can be verified by the the discontinuity of $\partial\Delta/\partial t$ across the transition point. The ground state becomes more complicated in Fig.6(b) where two critical values $t_{c1}/h_x=0.94$ and $t_{c2}/h_x=1.08$ are involved. Besides a first-order transition from the normal paring state to the nSF2 phase, the ground state changes to nSF1 state when the tunneling is above t_{c2}/h_x. We note that in this

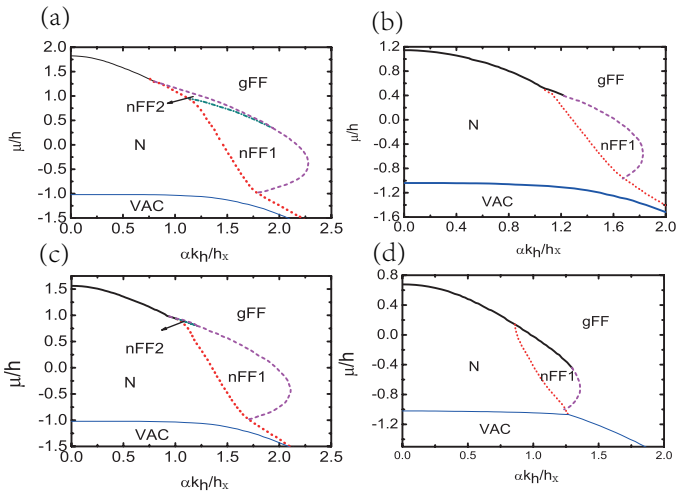

FIG. 7: Phase diagram of finite momentum paring state in $\alpha-\mu$ plane. We still analyze quantum phase with different interaction and different tunneling. For (a) and (b), the parameter is set as: (a).$g=-0.35$;(b).$g=-0.65$, respectively. The other parameter for the two figures are set as: $t=1, h_x=1, h=0.2$. For (c) and (d), the parameter is set as: (c).$t=0.9$; (d).$t=0.5$, respectively. The other parameters of the two figures are set as: $g=0.35, h_x=1; h=0.2$. In all the figures, the black solid lines represent the first-order phase transition boundaries while the dashed burgundy lines represent the continuous phase transition boundaries. The red dotted curve corresponds to $\Delta=10^{-3}$ threshold.

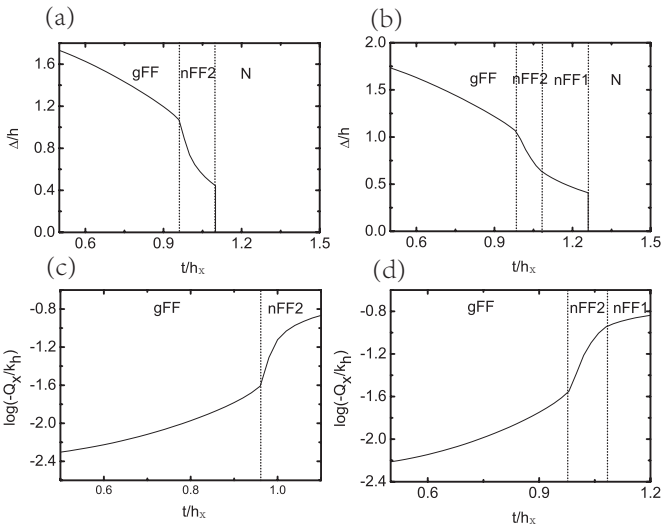

FIG. 8: Phase diagrams of the the paring order parameter δ and center-of-mass momentum Q_x with different tunneling t. The chemical potential μ and SOC strength in (a)/(c) and (b)/(d) is set as $\mu=0.6, \lambda k_h/h_x=1.25$ and $\mu=0.9, \lambda k_h/h_x=1.5$, respectively. The other parameters are set as follows: $g=-0.35, h_x=1, h=0.2$.

case, the transition is continuous which is also consistent with the results shown in Fig. 5.

B. FF PARING STATE WITH OUT-OF-PLANE ZEEMAN FIELD

When transverse Zeeman field is introduced, the presence of SOC leads to a asymmetric deformed Fermi surface. In this case, s-wave paring with zero center-of mass momentum becomes unfavorable, which is replaced with FF states with finite Q_x. Qualitatively, this corresponds to a shift about the local minimum of the thermodynamic potential from $Q_x=0$ to a finite Q_x plane. When the shift is small, most of the properties of the FF state are similar with the paring states with zero center-of-mass momentum.

In Fig.7, we map out the phase diagrams in the $\alpha-\mu$ plane with different interaction and different tunneling. The calculation shows that these diagrams share similar patterns shown in Fig. 5, except that the nodal superfluid states are now replaced by nodal FF states. We stress that in all these diagrams, FF state is hosted in the $\alpha-\mu$ plane. This is very different from the usual two dimensional polarized Fermi gases without SOC, where FFLO states can only be stabilized within a small parameter region. Therefore, FF states becomes more stable due to the presence of transverse Zeeman field and SOC, which greatly increases the possibility to find such exotic pairing states in our system.

Fig. 7(a) and 7(b) show the phase diagrams with different interactions. We can find the first order phase transition line is longer with larger interaction. In addition, nodal FF state is more favourable with smaller interaction. For instance, when interaction strength $g=-0.35$, there are two kinds of nodal-FF state, two-node FF state (nFF1) and four-node FF state (nFF2). As the interaction strength g increases, nFF2 disappears gradually and the regime for nFF1 phase also becomes smaller. It is expected that when the interaction is very strong, all the nodal FF states will be replaced by fully gapped FF states.

To illustrate the crossover physics of FF states, we also plot the phase diagrams for different tunnelings $t=(1, 0.9, 0.5)$, as shown in Fig. (7a), (7c) and (7d) respectively. When $t=(1, 0.9)$, both nFF1 and nFF2 phase appear in the phase diagram, although the region of nFF2 shrinks rapidly as t decreases. When the tunneling decreases to 0.5, only nFF1 is left in the phase diagram. Therefore, we assert that nFF2 is favourable with larger tunneling. In this case, the system is more appropriate to be treated as a two dimensional one. When tunneling decrease further, the situation becomes more complicated, and tFF state comes into play as shown in Fig. 2. Fig. 8 shows the changes of the pairing order parameter and center-of-mass momentum as we increase the inter-tube tunneling t. One can see that fully gapped FF state always exists in the dimensional crossover region,

while nodal FF state emerges around $t = 1$. The center-of-mass momentum $|Q_x|$ increases almost monotonically along with t. The ground state changes to normal state when t is larger enough.

V. CONCLUSION

In summary, we have studied the paring state in the dimensional crossover region in an array of coupling tubes. The interplay of SOC, Zeeman field, and tunneling lead to rich phase structure with exotic pairing states. In particular, the ground state is FFLO state with finite center-of-mass momentum pairing over large parameter region, which facilitates the experimental verification of this kind of exotic paring state. For quasi one dimensional system, there is tFF state in the phase diagram, which is characterized by the presence of Majorana edge state in the model. In order to qualitatively show the transition from the tFF state to normal SF state in the crossover region, a toy model composed of two-coupled tubes is studied to show the critical tunneling. Further more, the phase diagrams with different interaction and inter-tube tunneling are also presented. Except for fully gapped states, we find that there is a large parameter region for which pairing states with isolated gapless excitations in the dispersion appears. nSF and nFF states exist when the system is a quasi two dimensional system, and finally they change to normal state with further increasing the inter-tube tunneling.

Acknowledgments: We thank Wei Yi, Fan Wu, Bei-Bin Huang for helpful discussions. This work is supported by NSFC under Grant No. 11504038, " Chongqing Fundamental, Frontier Research Program" (Grant No. cstc2015jcyjA00013), and Foundation of Education Committees of Chongqing (Grant No. KJ1500411). X.-F Zhou acknowledges the support from the National Fundamental Research Program of China (Grants No. 2011CB921200 and No. 2011CBA00200), the Strategic Priority Research Program of the Chinese Academy of Sciences (Grant No. XDB01030200), and NSFC (Grant Nos. 11474266). L.Wen acknowledges the support from NSFC under Grant No. 11504037, " Chongqing Fundamental and Frontier Research Program" (Grant No. cstc2015jcyjA50024), and Foundation of Education Committees of Chongqing (Grant No. KJ1500311).

[1] D.Culcer, J.Sinova, N.A.Sinitsyn, T.Jungwirth, A.H.MacDonald, Q.Niu, Phys. Rev. Lett. **93**, 046602(2004)
[2] Q.-F.Sun, X.-C.Xie, Phys. Rev. B, **71**, 155321(2005)
[3] D.Hsieh, F.Mahmood, J.W.Mclver, D.R.Gardner, Y.S.Lee, N.Gedik, Phys. Rev. Lett, **107**, 077401(2011)
[4] M.Z.Hasan, C.L.Kane, Rev. Mod. Phys, **82**, 3045(2010)
[5] X.-L.Qi, S.-C.Zhang, Rev. Mod. Phys. **83**, 1057(2011)
[6] C.L.Kane, E.J.Mele, Phys. Rev. Lett. 95, 146802(2005)
[7] Y.-J.Lin, K.Jimenez-Garcia, and I.B.Spielman, Nature **471**, 83(2011)
[8] P.Wang, Z.-Q.Yu, Z.Fu, J.Miao, L.Huang, S.Chai, H.Zhai, and J.Zhang, Phys.Rev.Lett.**109**,095301(2012)
[9] L.W.Cheuk, A.T.Sommer, Z.Hadzibabic, T.Yefsah, W.S.Bakr, and M.W.Zwierlein, Phys.Rev.Lett.**109**,095302(2012)
[10] P.-J Wang, Z.-Q Yu, Z.-K Fu, J.Miao, L.-H Huang, S.-J Chai, H.Zhai, J.Zhang, Phys. Rev. Lett. **109**, 095301 (2012)
[11] Z.-K Fu, L.-H Huang, Z.-M Meng, P.-J Wang, X.-J Liu, H.Pu, H.Hu, J.Zhang, Phys. Rev. A **87**, 053619(2013)
[12] L.-H Huang, P.-J Wang, P.Peng, Z.-M Meng, L.-C Chen, P.Zhang, J.Zhang, arXiv:1504.02021(2015)
[13] L.-H Huang, Z.-M Meng, P.-J Wang, P.Peng, S.-L Zhang, L.-C Chen, D.H Li, Q.Zhou, J.Zhang, arXiv:1506.02861(2015)
[14] Z.-Q Yu, H.Zhai, Phys. Rev. Lett. **107**, 195305(2011)
[15] M.Gong, S.Tewari, and C.-W Zhang, Phys. Rev. Lett. **107**, 195303(2011)
[16] J.Zhou, W.Zhang, W.Yi, Phys. Rev. A **84**, 063603(2011)
[17] G.Chen, M.Gong, and C.-W Zhang, Phys. Rev. A. **85**, 013601(2012)
[18] L.-Y He, X.-G Huang, Phys. Rev. Lett. **108**, 145302 (2012)
[19] L.-Y He, X.-G Huang, Phys. Rev. B. **86**, 014511 (2012)
[20] L.-Y He, X.-G Huang, H. Hu, X.-J Liu, Phys. Rev. A. **87**, 053616(2013)
[21] J.P.Vyasanakere, S.-Z Zhang, V.B.Shenoy, Phys. Rev. B. **84**, 014512(2011)
[22] M.Gong, G.Chen, S.Jia, C.Zhang, Phys. Rev. Lett. **109**, 105302(2012)
[23] X.-J Liu, H.Hu, Phys. Rev. A. **88**, 023622(2013)
[24] H.Hu, L.Jiang, H.Pu, Y.Chen, X.-J Liu, Phys. Rev. Lett. **110**, 020401(2013)
[25] S.-G Peng, X.-J Liu, H.Hu, K.-J Jiang, Phys. Rev. A. **86**, 063610(2012)
[26] H.Hu, H.Pu, J.Zhang, S.-G Peng, X.-J Liu, Phys. Rev. A. **86**, 053627(2012)
[27] X.-J Liu, H.Hu, Phys. Rev. A. **85**, 033622(2012)
[28] X.-J Liu, L.Jiang, H.Pu, Hui Hu, Phys. Rev. A. **85**, 021603(R)(2012)
[29] L.Jiang, X.-J Liu, H.Hu, H.Pu, Phys. Rev. A. **84**, 063618(2011)
[30] M.Endres, T.Fukuhara, D.Pekker, M.Cheneau, P.Schauβ, I.Bloch, Nature, **487**, 454(2012)
[31] L.Pollet, N.V.Prokofev, Phys. Rev. Lett. **109**, 010401(2012)
[32] I.Bloch, J.Dalibard, W.Zwerger, Rev. Mod. Phys. **80**, 885(2008)
[33] L.-M.Duan, E.Demler, M.D.Lukin, Phys. Rev. Lett. **91**, 090402(2003)
[34] P.Fulde and R.A.Ferrell, Phys. Rev. **135**, A550(1964)
[35] A.I.Larkin and Y.N.Ovchinnikov, Zh. Eksp. Teor. Fiz. **47**, 1136(1964)
[36] H.A.Radovan et.al., Nature, **425**, 51(2003)
[37] A.Bianchi, R.Movshovich, C.Capan, P.G.Pagliuso, and

J.L.Sarrao, Phys. Rev. Lett. **91**, 187004(2003)
[38] K. Kakuyanagi, et al., Phys. Rev. Lett. **94** 047602(2005)
[39] S.Uji, H.Shinagawa, T.Terashima, T.Yakabe, et.al., Nature **410**, 908(2001).
[40] Y.Liao, A.S.C.Rittner, T.Paprotta, W.-H.Li, G.B.Partridge, R.G.Hulet, S.K.Baur and E.J.Mueller, Nature **467**, 567(2010).
[41] W.Ketterle and M.W.Zwierlein, arXiv.org:0801.2500
[42] Y.L.Loh and N.Trivedi, Phys. Rev. Lett. **104**, 165302(2010)
[43] M.M.Parish, S.K.Baur, E.J.Mueller, and D.A.Huse, Phys. Rev. Lett. **99**, 250403(2007).
[44] J.M.Edge and N.R.Cooper, Phys. Rev. Lett. **103**, 065301(2009).
[45] K.Yang, Phys. Rev. Lett. **95**, 218903(2005).
[46] C.-L Qu, Z.Zheng, M.Gong, et.al., Nature Communication **4**, 2710(2013)
[47] W.Zhang, W.Yi, Nature Communication **4**, 2711 (2013)
[48] X.-J Liu, H.Hu, Phys. Rev. A **88**, 023622 (2013)
[49] Y.Cao, S.-H Zou, X.-J Liu, et.al., Phys. Rev. Lett. **113**, 115302(2014)
[50] K.Sun, C.J. Bolech, Phys. Rev. A **87**, 053622 (2013)
[51] M.Z.Hasan and C.L.Kane, Rev. Mod. Phys. 82, 3045 (2010)
[52] L.-M.Duan, E.Demler, M.D.Lukin, Phys. Rev. Lett. **91**, 090402(2003)
[53] A.Y.Kitaev, Ann. Phys. **321**, 2111(2003)